Sorption Phenomena In Transient Vapor Intrusion Scenarios

Jonathan G. V. Ström[a], Shuai Xie[a], Eric M. Suuberg[a]

These authors contributed equally to this work

[a]*Brown University, School of Engineering, Providence, RI, USA*

Abstract

Many vapor intrusion (VI) contaminants have the capacity to sorb onto a variety of materials commonly found in buildings as well as soils, yet the role and effect of sorption in VI is largely unstudied. To bridge this gap we measure the sorptive capacities of trichloroethylene (TCE) on some materials at VI relevant concentrations; finding that material sorptive capacities vary orders of magnitudes, with cinderblock having a capacity to hold up to almost 14,000 times more contaminant than a comparable TCE contaminated air volume. Using these experimentally derived data together with a three-dimensional numerical model of VI, we then explore the retarding effect that sorption has on contaminant transport in soils and indoor environments. We also apply the model to investigate how the contaminant desorption from these materials, following the implementation of a successful VI mitigation scheme, affect contaminant expulsion. We find that desorption may cause significant delay: in some cases taking months longer than if there were no sorbed contaminants.

Keywords: Vapor intrusion, Temporal variability, Sorption, Attenuation factor, Mitigation

1. Introduction

Most vapor intrusion (VI) contaminants have the capacity to sorb onto soil and various common indoor materials, but the role and more importantly, the consequences of these sorption processes in VI are poorly understood[1, 2, 3]. The migration of contaminant vapors from their source into the VI impacted building and potential indoor sources is usually the prime concern

in VI investigations. Rarely are the sorbed contaminant vapors in the soil or indoor considered in an investigation. These may potentially act as a capacitance, storing and releasing contaminant vapors in response to a change in contaminant concentration. Consequently, contaminant vapors may be more persistent than expected at a site that has undergone remediation, potentially reducing the effectiveness of mitigation in the short term, or leading to misleading results regarding mitigation efficacy.

It is well recognized that building materials have the capacity to sorb pollutants. The sorptive capacity of various volatile organic compounds (VOCs) of concern in VI has been examined on a variety of building materials, such as particle density board[4], gypsum wallboard[5], and plywood and carpets[6]. However, most of these studies used relative high contaminant concentrations, usually around mg/m^3[4] or even higher. This is several orders of magnitude higher than the concentrations relevant in VI and due to the nonlinear nature of sorption with respect to concentration, sorption studies at lower concentration are needed.

Many VOC sorption studies have also focused on the interaction between building materials and formaldehyde[5], toluene, and decane[6]. However, one of the contaminants of greatest concern in VI - trichloroethylene (TCE), has not received attention. This is despite the fact that sorption of TCE (and other comparable VOCs) on activated carbon is extensively used to treat indoor air contamination and their sorption on passive tube samplers is widely employed for analysis of these compounds[7].

Over the years many VI sites have been investigated. Two well-known examples of these are the studies of a house in Layton, Utah and one in Indianapolis, Indiana. Both of these sites were outfitted with a wide variety of instrumentation to measure various metrics such as contaminant concentration in interior, soil, and groundwater, as well as pressure, temperature, or weather. These studies yielded some of the richest VI datasets available and gave invaluable insights into the VI process, including into the application of CPM[8] and sub-slab depressurization (SSD) mitigation systems[9, 10]. However, neither of these studies considered the role that sorption may have had at these sites.

The potential impact of sorption could perhaps be most significant in situations in which contaminant entry rates vary widely with time, such as in the application of the controlled pressure method (CPM) and various mitigation schemes. The controlled pressure method involves the forced over- and depressurization of a building to maximize or minimize the contaminant entry

rate into the building. This can help the investigator ascertain the worst-case VI scenario and help identify potential indoor contaminant sources[11, 8]. However, if the building indoor materials have a large sorptive capacities, then desorption and sorption processes may significantly affect the indoor air contaminant concentration. Likewise, a significant amount of sorbed contaminant may be released from interior materials over an unknown period of time after mitigating the contaminant intrusion at a site[1, 2].

In the past, VI models have been used to gain further insight into VI processes. Previous examples of VI modeling studies include one on the role of rainfall in VI[12], or drivers of temporal variability in some of the aforementioned sites[13]. However, while many VI models are presented including a sorption term in the governing equation for contaminant transport in soils, none have really explored the role of sorption in VI in a transient simulation. The reason for this is two-fold. First, there has been a general lack of interest in sorption related to VI thus far. Secondly, the vast majority of VI modeling efforts and studies have focused on steady-state analyses of VI, and sorption only affects soil contaminant transport in time-dependent scenarios.

To bridge this knowledge gap we will explore the role of sorption in VI by considering the signifnance of newly obtained contaminant sorption data in the context of VI models. Sorption data of TCE on various materials, including cinderblock, drywall, wood, paper, carpet, and Appling soil have been measured in a fixed bed sorption experiment. These sorption data are used to generate sorption parameters to be used in a three-dimensional finite element VI model. For this purpose we will consider a prototypical VI scenario where a free-standing house, with a basement, is overlying a homogenously contaminated groundwater source. Using this model we investigate how contaminant transport is affected by sorption, how indoor sorptive materials affect indoor air concentration as the building's pressurization fluctuates and how indoor air concentration are affected by indoor materials following successful mitigation of the structure.

2. Methods

2.1. Experimental Setup

The details of the experiments used in obtaining the sorption input data will be discussed i na seaprate paper being prepared on this topic. Here, we only briefly summarize the experiments.
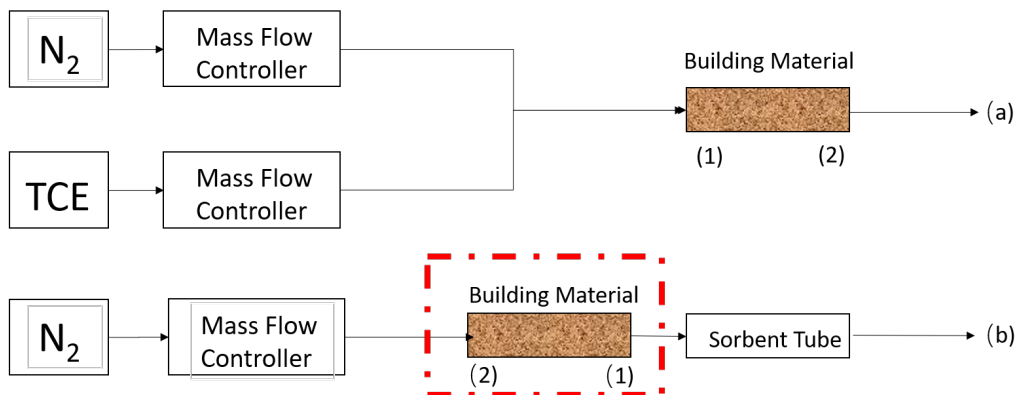
3

Figure 1: Schematic of experimental setup.

To study the dynamic sorption of TCE onto the selected building materials, the two-step process shown in Figure 1 was used.

A 7.5 by 1.27 cm stainless steel column was filled with a ground sample of the material to be tested. We use 2.0 g of drywall, and 1.0 g of all the other materials to pack the tube. Samples were held in by glass wool plugs. Using flow controllers, TCE was diluted in nitrogen gas to 1.12 ppb$_v$ and flowed through the column at a rate of 60 mL per minute, for a pre-selected time period. After the material had been exposed for the selected time, the column was detached and attached to the desorption system.

In the desorption system, the sample-containing column was heated to 100 °C and pure nitrogen gas was flowed through the previously outlet side of the column - carrying the desorbed contaminant with it. The gas was then passed through a long tube, allowing the gas to cool to room temperature, from which it flowed into a carbon-filled stainless steel sorption column which trapped all of the TCE for analysis. The sorption column was then desorbed into a gas-chromatograph fitted with a electron capture detector.

2.2. Numerical Model

To investigate the role of sorption in VI, we developed a three-dimensional numerical model of a building overlying a TCE contaminated groundwater source in the commercial finite-element solver COMSOL. The building is assumed to have a 10 by 10 m footprint, with a 3 meter ceiling height, and its foundation is located 1 m below ground surface (bgs). The contaminated groundwater is 4 m bgs, and is assumed to be homogenously contaminated with TCE. The building is surrounded by homogenous soil, that extends 10

4

Figure 2: The vapor intrusion model. Not yet done.

m from its walls. Along the perimeter of the foundation, there is a 1 cm wide crack through which contaminant vapors enter the building and expulsion of contaminant vapors from the indoor occurs through air exchange with the outside.

Contaminant vapors are transported from the contaminated groundwater through the soil matrix via advection and diffusion and is described in 2.2.3. The presence of the groundwater variably saturates the soil matrix with water, which has a significant effects on the contaminant transport and is modeled using van Genuchten's retention model[14] and explained in greater detail in section 2.2.1. The water in the soil matrix is assumed to be stationary, thus advective transport only occurs through the vapor phase, while diffusion occurs through both the water and the vapor phases. The contaminant vapors are also assumed to be able to sorb onto the soil particles, and is modeled using a linear sorption model, and the interaction between the water and vapor phases are determined by Henry's Law.

The building is assumed to be pressurized relative to the outside, which gives an air flow in and out of the building (depending on if it is depressurized or overpressurized). This air flow causes the advective contaminant transport through the soil and the foundation crack. Darcy's Law is used to model the flow of air and is described in detail in section 2.2.2. A key assumption here is that the contaminant is so diluted in the air, that it is assumed to not affect the transport properties of air.

In our implementation, only the soil surrounding the building is explicitly modeled (as a three-dimensional geometry), and the interior of the basement is implicitly modeled as a continuously stirred tank reactor as described in section 2.2.4. These two are coupled via the foundation crack, from which the contaminant entry into the basement is calculated, and contaminant expulsion is determined by the air exchange rate. In this work we consider the role of sorption on materials in the interior, which is done as a equilibrium reaction.

An overview of this modeling approach may be seen in Figure 2.

2.2.1. Vadose Zone Moisture Content

Since the contaminant transport occurs through the three-phase vadose zone, it is important that we correctly account for soil moisture content and

5

its effect on advective and diffusive transport. In this modeled scenario, we assume that the soil moisture is at steady-state, and thus the soil moisture content is given by the retention model developed by van Genuchten[14].

The van Genuchten retention model gives the soil water saturation as a function of elevation above groundwater. This in turn gives the water and gas filled porosities in the soil, and the relative permeability of the soil matrix.

$$\text{Se} = \begin{cases} \frac{1}{(1+\alpha z^n)^m} & z < 0 \\ 1 & z \geq 0 \end{cases} \tag{1}$$

$$\theta_w = \begin{cases} \theta_r + \text{Se}(\theta_s - \theta_r) & z < 0 \\ \theta_s & z \geq 0 \end{cases} \tag{2}$$

$$k_r = \begin{cases} \text{Se}^l \left[1 - \left(1 - \text{Se}^{\frac{1}{m}} \right) \right]^2 & z < 0 \\ 0 & z \geq 0 \end{cases} \tag{3}$$

Se is the saturation, and ranges from 0 to 1, which represent completely unsaturated to fully saturated; z is a height relative to groundwater in meters, with $z = 0$ the groundwater surface and $z < 0$ into the vadose zone; θ_r, θ_s, θ_w, and θ_g are the dimensionless porosity parameters reflecting the residual moisture content, saturated porosity (or just porosity), and water and air filled porosities respectively; k_r is the relative permeability of water transport and $1 - k_r$ gives the relative permeability of air transport.

2.2.2. Gas Flow In The Vadose Zone

The gas flow in the vadose zone is governed by a modified version of Darcy's Law. Originally, Darcy's Law was developed to describe flow in saturated porous media; but flow in unsaturated media requires some modification. An effective permeability that depends on the relative permeability given by the van Genuchten equations is introduced to allow for correct permeability in unsaturated porous media.

The vapor flow continuity governing equation is given by

$$\frac{\partial}{\partial t}(\rho \theta_s) + \nabla \cdot \rho \left(- \frac{(1 - k_r)\kappa}{\mu} \nabla p \right) = 0 \tag{4}$$

Here ρ is the fluid density; κ is the saturated permeability of the soil matrix; μ is the fluid viscosity; and p is the fluid pressure. We assume that the contaminant vapors are so dilute that the gas flow properties can be taken to be those of air, specifically at 20 °C. All the transport properties may be found in Table 1.

6

Boundary Conditions. To solve (4) we assign the atmosphere boundary (see Figure 2) to be the reference pressure, i.e. zero pressure. The foundation crack boundary is assigned to be at the indoor-outdoor pressure difference value. Remaining boundaries are no-flow boundary conditions.

$$\text{Atmosphere} \qquad\qquad p = 0 \ (\text{Pa}) \qquad\qquad (5)$$

$$\text{Foundation crack} \qquad p = p_{\text{in}} - p_{\text{out}} = p_{\text{in}} \ (\text{Pa}) \qquad (6)$$

$$\text{All other} \qquad\qquad -\vec{n} \cdot \rho_{\text{air}} \vec{u} = 0 \ (\text{kg}/(\text{m}^2 \cdot \text{s})) \qquad (7)$$

Here $\vec{n}$ and $\vec{u}$ are the boundary normal and gas velocity vectors.

Initial Conditions. For steady-state problems, the initial conditions do not influence the solution. Transient simulations however, require initial conditions and these are assumed to be given by the steady-state solution.

2.2.3. Mass Transport In The Vadose Zone

Contaminants in the vadose zone exist in three phases - gaseous, dissolved in water, and sorbed onto soil particles. While there are three distinct phase concentrations, the water and gas phases are related via Henry's Law (8).

$$c_g = K_H c_w \qquad\qquad (8)$$

Where c_g and c_w are the gas and water phase concentrations respectively in mol/m^3; K_H is the dimensionless Henry's Law constant.

In this work, we consider sorption equilibrium between the soil and vapor phases, to be governed by the water contaminant concentration (9).

$$c_s = K_{\text{ads}} \rho_b c_g = K_{\text{ads}} \frac{\rho}{1 - \theta_t} K_H c_w \qquad\qquad (9)$$

Here the c_s is the solid phase concentration in mol/kg; ρ_b is the bulk density of the soil kg/m^3, which is given by the density ρ and the total soil porosity θ_t; K_{ads} is the vapor-solid sorption partition coefficient in m^3/kg.

Mass transport in the vadose zone is governed by diffusion and advection and is given by (10). It is important to note that this governing equation is written in terms of the water phase contaminant concentration c_w, but via Henry's Law and the vapor-solid sorption partition coefficient, it does in fact describe the contaminant concentration and transport in all three phases.

$$R \frac{\partial c_w}{\partial t} = \nabla \cdot [D_{\text{eff}} \nabla c_w] - K_H \vec{u} \cdot \nabla c_w \qquad\qquad (10)$$

The first term in (10) gives the change in contaminant water concentration with respect to time, modified by the *retardation factor*, R, which is discussed below; The second is the effective diffusive flux which is modified by the effective diffusion coefficient D_{eff} which is also discussed below. The third is the advective flux where $\vec{u}$ is the soil-gas velocity from Darcy's Law, which when multiplied with K_H gives the gas phase concentration advective flux, e.g. advective transport only occurs in the vapor phase and not the liquid phase (the water in the soil matrix is assumed to be at steady-state).

Contaminant entry into the building. The contaminant enters the building through a combination of advection and diffusive fluxes and is given by (11).

$$j_{ck} = \begin{cases} u_{ck}c_g - \frac{D_{\text{air}}}{L_{\text{slab}}}(c_{in} - c_g) & u_{ck} \geq 0 \\ u_{ck}c_{in} - \frac{D_{\text{air}}}{L_{\text{slab}}}(c_{in} - c_g) & u_{ck} < 0 \end{cases} \tag{11}$$

Here the j_{ck} is the molar contaminant flux into the building in $\text{mol}/(\text{m}^2 \cdot \text{s})$; D_{air} is the contaminant diffusion coefficient in pure air in m^2/s; L_{slab} is the thickness of the foundation slab in m. The flux expression changes if there is a bulk flow into the building, i.e. $u_{ck} \geq 0$, or out of the building.

Retardation factor. As the contaminants are transported through the vadose zone, the partitioning between the various phases increases the contaminant residency time, retarding the transport of contaminants. This effect is represented by R which is the retardation factor (12).

$$R = \theta_w + \theta_g K_H + \rho_b K_H K_{\text{ads}} \tag{12}$$

Here θ_w, θ_g are the water and gas filled soil porosities; K_{ads} is the vapor-solid partition coefficient in m^3/kg.

Effective diffusivity. The effective diffusivity in the vadose zone varies with the soil moisture content, from being close to that in water when fully saturated and close to that in air when soil moisture is low. Millington-Quirk developed (13) which describes the effective diffusivity in variably saturated porous media.

$$D_{\text{eff}} = D_{\text{water}} \frac{\theta_w^{\frac{7}{3}}}{\theta_t^2} + \frac{D_{\text{air}}}{K_H} \frac{\theta_g^{\frac{7}{3}}}{\theta_t^2} \tag{13}$$

Where the porosity terms reflect the water and gas phase tortuosity; D_{air} and D_{water} are the contaminant diffusion coefficient in air and water respectively in m^2/s; The Henry's Law constant K_H appears here to reflect that all the contaminant transport is a function of the contaminant water concentration.

8

Boundary Conditions. In this model, the sole contaminant source is assumed to be the homogenously contaminated groundwater, which we assume to have a fixed concentration. The atmosphere acts as a contaminant sink and thus this is simply a zero concentration boundary condition. Contaminants leave the soil domain and enter the building through a combination of advective and diffusive gas phase transport. The boundary condition applied to all other boundaries is a no-flow boundary.

$$\text{Groundwater} \qquad\qquad c_w = 0 \text{ (mol/m}^3) \qquad (14)$$

$$\text{Atmosphere} \qquad\qquad c_w = c_{gw} \text{ (mol/m}^3) \qquad (15)$$

$$\text{Foundation crack} \qquad -\vec{n} \cdot \vec{N} = -\frac{j_{ck}}{K_H} \text{ (mol/(m}^2 \cdot \text{s))} \qquad (16)$$

$$\text{All other} \qquad -\vec{n} \cdot \vec{N} = 0 \text{ (mol/(m}^2 \cdot \text{s))} \qquad (17)$$

$\vec{n} \cdot \vec{N}$ is the dot product between the boundary normal vector and the contaminant flux; $j_c k$ is the contaminant vapor flux into the building. We assume that only contaminants in the gas phase enter the building, and dividing j_{ck} by K_H we get proper accounting in terms of the water phase concentration accounting in the main transport equation 10.

Initial Conditions. For transient simulations in this work, the steady-state solution to a corresponding case is always used as an initial condition.

2.2.4. Indoor Environment

The indoor air space is modeled as a continuously stirred tank reactor (CSTR) given by (29). Contaminants are assumed to only enter through the foundation crack, represented by n_{ck}, which is calculated by integrating the contaminant flux over the foundation crack boundary. The product of air exchange rate, (which governs how many house volumes are exchanged with the outside per time unit,) and indoor air contaminant concentration gives the contaminant exit rate fromthe house. The sorption of contaminant on indoor materials is given by the sorption term in (31) and the sorbed contaminant concentration on all interior surfaces is given by (30).

9

$$V_{\text{bldg}}\frac{\partial c_{\text{in}}}{\partial t} = n_{\text{ck}} - A_e c_{\text{in}} V_{\text{bldg}} - r_{\text{sorb}} V_{\text{mat}} \tag{18}$$

$$V_{\text{mat}}\frac{\partial c_{\text{sorb}}}{\partial t} = r_{\text{sorb}} V_{\text{mat}} \tag{19}$$

$$r_{\text{sorb}} = k_1 c_{\text{in}} - k_2 c_{\text{sorb}} \tag{20}$$

$$n_{\text{ck}} = \int_{A_{ck}} j_{ck} dA \tag{21}$$

Here V_{bldg} and V_{mat} are the indoor control volume and volume of indoor material in m^3; c_{in} and c_{sorb} are the indoor and sorbed (onto the indoor material) contaminant concentrations in mol/m^3; n_{entry} is the contaminant entry rate in mol/s, which is calculated by integrating the contaminant flux j_{ck} over the foundation crack area; r_{sorb} sorption rate in mol/(m$^3 \cdot$ s); k_1 and k_2 are the sorption and desorption rate constants in 1/s.

Fitting Kinetic Parameters. These values of k_1 and k_2 are found by applying (31) numerically to the experimental data via least square fitting. We use Runge-Kutta method of order 5(4) as the numerical solve, which is implemented together with the least square method in the SciPy python package[15].

Soil Properties[? 16, 17]						
Soil	κ (m^2)	θ_s	θ_r	α (1/m)	n	ρ kg/m^3
Sand	$9.9 \cdot 10^{-12}$	0.38	0.053	3.5	3.2	1460
Sandy Loam	$5.9 \cdot 10^{-13}$	0.39	0.039	2.7	1.4	1460
Trichloroethylene (diluted in air) Properties[16, 17]						
D_{air} (m^2/h)	D_{water} (m^2/h)	ρ (kg/m^3)	μ (Pa $\cdot$ s)	K_H		
$2.47 \cdot 10^{-2}$	$3.67 \cdot 10^{-6}$	1.614	$1.86 \cdot 10^{-5}$	0.403		
Building Properties						
V_{base} (m^3)	L_{slab} (cm)	A_e (1/hr)				
300	15	0.5				

Table 1: Transport and material properties used in the model. See Table 4 for nomenclature.

3. Results & Discussion

3.1. Fitting Sorption Parameters

Figure 3 shows the result of fitting the sorption data for three select materials - wood, Appling soil, and cinderblock concrete. The k_1 and k_2 represent the rates at which TCE sorbs and desorbs respectively onto/from the material of interest. The equilibrium partition constant, using the formulation in (31), is given by

$$K = \frac{k_1}{k_2} \tag{22}$$

and defines the sorption isotherm. Here a larger K indicates that there is a greater propensity for contaminant sorption.

To apply a soil sorption isotherm in (10) K needs to be converted to m^3/kg. This is done by multiplying K isotherm with inverse of the soil bulk density ρ_b, which is taken to be 1460 kg/m^3.

$$K_{ads} = \frac{K}{\rho_b} = 5.28 \ (m^3/kg) \tag{23}$$

Table 2 shows the fitted parameters for the tested materials. Based on this these results we can see that cinderblock and soil have orders of magnitude larger sorption capacities than wood or drywall does. We can also see by that soil and cinderblock sorb quickly, much faster than a material with similar sorptive capacity such as paper.

Table 2: Fitted kinetic sorption parameters based on sorption experiment data. Six different types of materials are considered. k_1 and k_2 are the sorption and desorption constants respectively, and K is the sorption equilibrium constant.

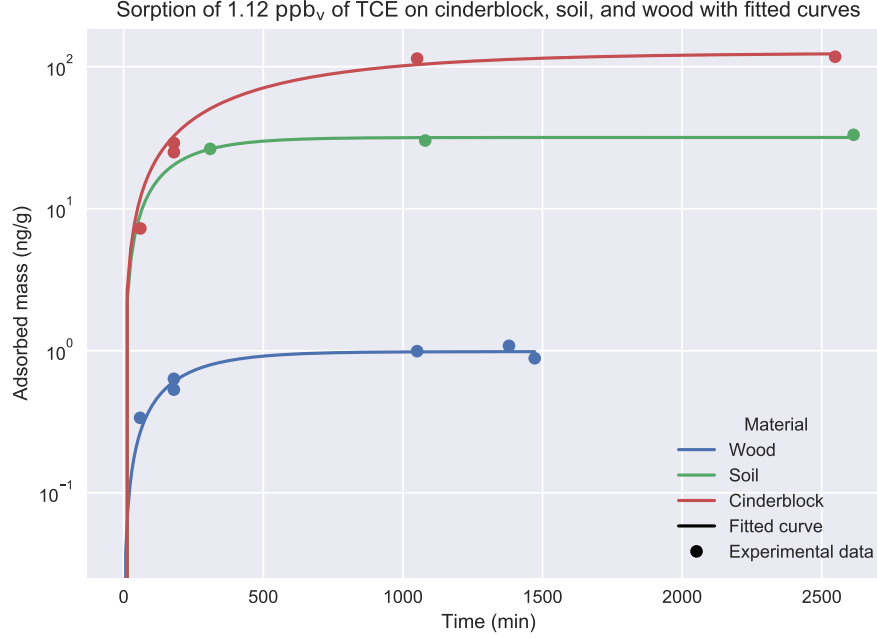| Material	k_1 (1/hr)	k_2 (1/hr)	K
Wood	44.90	0.32	140.90
Drywall	87.94	0.41	214.87
Carpet	58.74	0.26	226.21
Paper	88.37	0.04	2195.69
Soil	2636.57	0.34	7702.94
Cinderblock	4175.16	0.10	41501.26

Figure 3: Experimental data of sorption of TCE onto three select materials as well as fitted sorption rates based on the kinetic model (31).

3.2. Soil Sorption's Retarding Effect

The effect of building pressurization is a key factor in VI that influences the advective contaminant transport into or out of the building. The magnitude of indoor contaminant concentration change in response to a pressurization change is significantly influenced by a variety of factors, such as soil permeability, foundation depth, soil moisture, and sorption. To investigate the effect that soil sorption has on contaminant soil mass transport in the VI context, we have run two types transient simulation where initially the modeled structure is depressurized at a steady -5 Pa to establish a steady-state baseline. At the start of the simulation, the building building is further depressurized to -15 Pa (24), or overpressurized to 15 Pa (25), and

the simulation is allowed to run for 72 hours.

$$\text{Depressurization}: \ p_{\text{in}} = \begin{cases} -5, & t = 0 \ (\text{hr}) \\ -15, & 0 < t \le 72 \ (\text{hr}) \end{cases} \tag{24}$$

$$\text{Overpressurzation}: \ p_{\text{in}} = \begin{cases} -5, & t = 0 \ (\text{hr}) \\ 15, & 0 < t \le 72 \ (\text{hr}) \end{cases} \tag{25}$$

For each of these cases, the simulation is run using two different soil types - sand and sandy loam. Sand is assumed here to not sorb any TCE, while for sandy loam a range of sorption isotherms are used. These range from no sorption ($K_{\text{ads}} = 0 \ (\text{m}^3/\text{kg})$) to the experimentally determined sorption isotherm for Appling soil ($K_{\text{ads}} = 5.28 \ (\text{m}^3/\text{kg})$). With the experimentally determined isotherm, we see that the ratio between sorbed concentration and soil-gas phase concentration is 7708, i.e. there is a much larger amount of contaminant sorbed to the soil than present in the vapor phase of the vadose zone. When $K_{\text{ads}} = 5.28 \cdot 10^{-4} \ (\text{m}^3/\text{kg})$ this ratio is roughly unity (0.77).
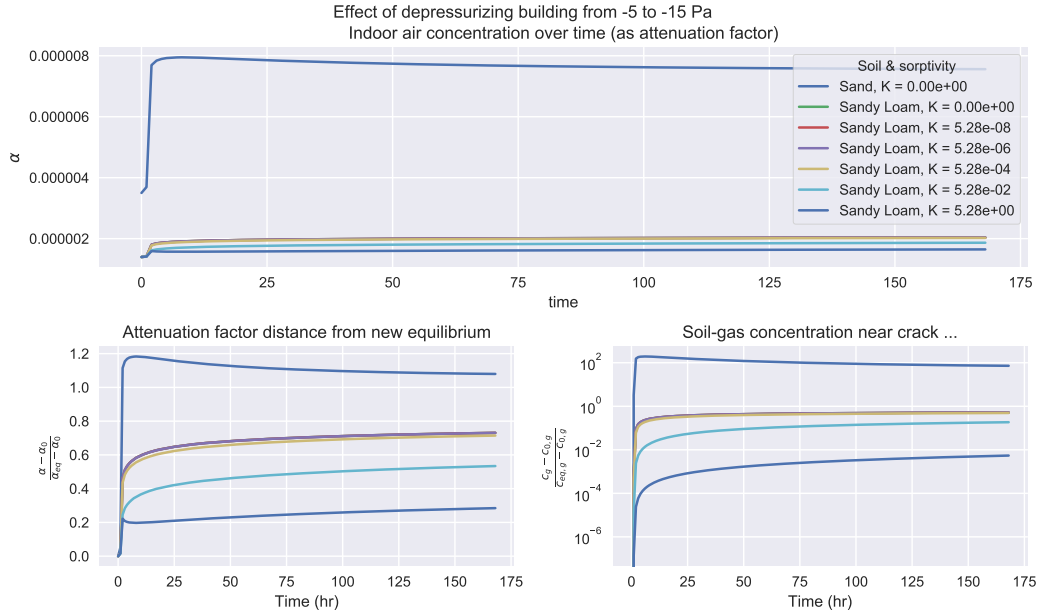

Figure 4

The top panel of Figure 4 shows the indoor air contaminant concentration as the simulated building is undergoing the depressurization as represented

13

by the equation (24) case. results are plotted as attenuation of contaminant relative to the groundwater source, i.e.

$$\alpha = \frac{c_{\text{in}}}{c_{\text{gw}} K_H} \tag{26}$$

Here we can see that when the surrounding soil consists of sand, the indoor concentration increases rapidly as the building is depressurized. The increase is significantly smaller for the sandy loam cases, and becomes smaller as the sorbed mass increases (K_{ads} increases).

The bottom left panel shows the time for reaching the new equilibrium. At the start of the simulation, the building starts at an attenuation of α_0, which is the steady-state concentration when the building is depressurized to -5 Pa. As the building is further depressurized to -15 Pa, the indoor air concentration will approach a new equilibrium state α_{eq} (the result of which is obtained from a steady-state simulation at that depressurization). By plotting $\frac{|\alpha - \alpha_0|}{|\alpha_{eq} - \alpha_0|}$ we can see how far away we are from the new equilibrium state, and a value of 0 represents that we are at the initial concentration, i.e. $\alpha = \alpha_0$, and a value of 1 represents $\alpha = \alpha_{eq}$, i.e. that the new equilibrium has been reached. This demonstrates that times of hundreds of hours may be needed to attain a near steady-state

The results of the same calculations are shown in the bottom right panel as well, but instead of plotting the indoor air concentration, we consider the average soil-gas concentration in a 5 cm diameter cylinder that envelops the entire perimeter crack. The choice of 5 cm is arbitrary, but helps illustrate what happens in the near-foundation-crack region. Examining these changes allow us to better understand how the contaminant is transported into the building from the soil. Consistent with the long timescales for the indoor air to "adjust" to a new condition, the soil which is a significant source/sink for the contaminant share a similar slow adjustment.

Before discussing the role of sorption, we can first compare the non-sorbing sand and sandy loam cases. Due to its higher permeability and lower moisture content, sand is significantly more permeable to gas flow than sandy loam (see Table 1 for permeability values). Consequently the advective transport through the foundation crack is much more significant in the sand case than the sandy loam case. This may be characterized by a Péclet number for transport through the foundation crack, where

$$\text{Pe} = \frac{\text{advection}}{\text{diffusion}} = \frac{u_{\text{ck}} L_{\text{slab}}}{D_{\text{air}}} \tag{27}$$

14

and the Péclet number is around 4 versus 0.2 at a -15 Pa depressurization for sand and sandy loam respectively. A Péclet greater than one indicate that advective transport dominates and vice versa.

Due to the advection dominated transport mechanism in the sand case, the indoor air concentrations are temporarily elevated above the final equilibrium concentration at -15 Pa. (Note that the absolute distance from equilibrium is plotted in Figure 4 which is why the concentration is two order of magnitude dispalced.) This phenomena occurs because initially more contaminants are drawn into the building from the near crack area than can be resupplied, temporarily depleting the local soil-gas contaminant concentration.

One can notice that many of the sandy loam lines overlap, and start diverging from each other when $K_{\mathrm{ads}} = 5.28 \cdot 10^{-4}$ (m^3/kg), at the point where the ratio of sorbed and soil-gas concentration are roughly equal. Since the indoor air concentration depend on the soil-gas concentration, this is the origin of the difference.

The reason for this is that it is at this threshold the that sorptive contribution to the retardation factor (12) starts to becomes larger than the other terms.

$$\rho_b K_H K_{\mathrm{ads}} > \theta_w + \theta_g K_H \tag{28}$$

Thus it is at this point that the contaminant transport, i.e. replenishment from the source in the soil starts to become retarded by sorption. The partitioning between the various phases controls residence time as the contaminant is transported. Under VI conditions, the values of $\theta_w + \theta_g K_H$ are relatively small values, while K_{ads} can vary by orders of magnitude, making sorption potentially a very significant retarder for soil transport.

We can also note that the retarding effect of sorption also somewhat depends on the contaminants Henry's Law constant K_H, bulk density ρ_b and the moisture content θ_w. For instance if the local temperature is higher, then contaminant K_H is likewise larger, and the retardation factor is greater. Generalizing this is difficult however, as K_{ads} decreases with temperature, and the interplay between these may be complicated. Nevertheless this hints that there may be a climate/weather component to how significantly sorption induced retardation is.

Figure 5 shows the same sort of analysis as in Figure 4 but with the building pressurization as described by (25). As the building is overpressurized, the indoor contaminant is pushed back out into the soil. Since the

15

indoor air concentration is lower than the soil-gas concentration, a drop in local soil-gas concentration is observed along with a decrease in indoor air contaminant concentration.
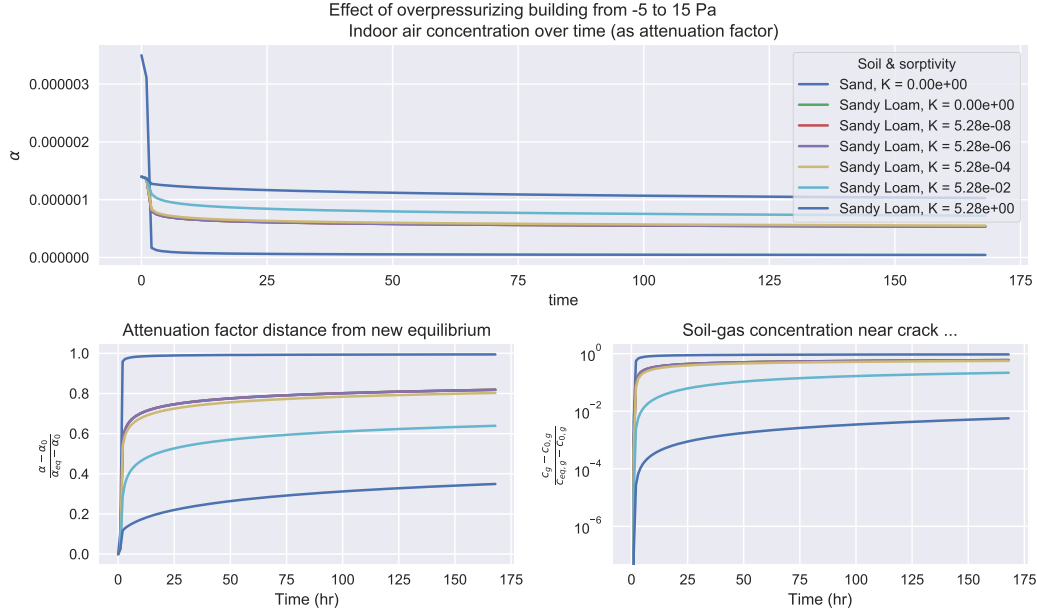

Figure 5

3.3. Effects of Indoor Material Sorption

For these simulations we assume that there is no soil sorption. We consider the basement (the indoor air space) and assume that the inside surfaces are entirely made up of one of the materials we presented in 3.1. We also assume that the material covering the indoor surfaces has a certain thickness or depth that the contaminants can penetrate - providing a certain volume or mass of sorbing material in the indoor environment. Table 3 shows the surface area, penetration depth, and volume of each material studied. While the assumptions regarding coverage of different portions of the space are arbitrary, they are of the right order of magnitude and they do present some limiting cases of the potential effect of sorption onto/from these materials.

The modeled building then undergoes a pressurization cycle, in which at start of the simulation it has been depressurized at -5 Pa at steady-state. The building is then sequentially depressurized to -15 Pa, then pressurized to

Material	d_{p} (mm)	V_{mat} (m^3)
Cinderblock	5	1.6
Wood	1	0.32
Drywall	10	3.2
Carpet	10	3.2
Paper	0.1	0.032

Table 3: The assumed contaminant penetration depth and subsequent volume of the sorbing indoor materials. The material surface area is assumed to be the same, and each material completely cover the surfaces of a 10x10x3 meter room.

15 Pa, and finally again depressurized to -5 Pa. For each sequence, the new pressurization is maintained for 24 hours. This pressurization cycle may be seen in the top left panel of 6. The choice of pressurization cycle is somewhat arbitrary, but can be used to represent limiting cases of natural pressurization variation, or artificially induced pressurization. Figure 6 shows the result of these simulations.

The change in indoor air contaminant concentration over this pressurization cycle is shown in the bottom panel of Figure 6. First we consider the reference case - where there is no sorbing indoor materials present. (The blue line is the reference case, which may be difficult to see as the wood and carpet lines overlap.) Here we see that as the building is depressurized, the indoor air contaminant concentration increases quickly in response to the depressurization change, and is approaching a new equilibrium.

The presence of the various studied building materials in the indoor environment have very different effects on the change in indoor air contaminant concentration. The presence of wood and carpet has little effect on the indoor air concentration, whereas cinderblock has a very significant effect, dampening out almost any change in indoor concentration. Drywall and carpet significantly delay the rate of change in the indoor concentration, but for each 24 hour cycle, roughly the same indoor concentration is reached as in the no sorbing material reference case.

The disparity in these result is explained by the the top right panel of Figure 6. Here the de- and sorption rates in μg/hr for each indoor material is shown. A positive and negative value here indicate that contaminant is desorbed from or sorbed to the material respectively. To understand this figure, it is useful to refer back to Table 2 which shows the sorption and
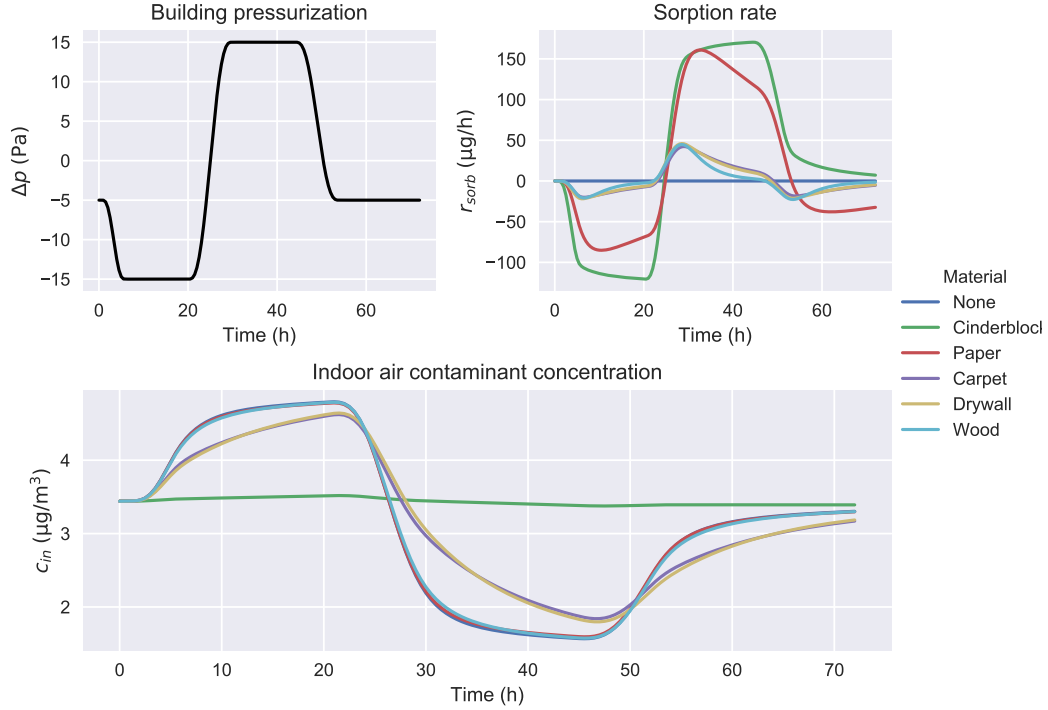
17

Figure 6: Comparison of how sorption onto/from various indoor materials affect the indoor air contaminant concentration (bottom) of a building that undergoes a pressurization cycle (top left). The rate of de- and sorption for each considered material during the cycle are also shown (top right) and is governed by (31). A positive value means that contaminant vapors are being sorbed onto/into the material and a negative means the material is desorbing into the indoor air space.

desorption rate constant k_1 and k_2 respectively, and the sorption equilibrium constant K (a larger value indicate a larger sorptive capacity).

First we consider to the depressurization part of the cycle (1-25 hours). As in the indoor concentration panel, we see that the wood, drywall, and carpet cases overlap. These materials have similar sorptive capacities (K) and sorptive rates (k_2). Paper, by contrast, has a similar shape to the previous three but its magnitude is significantly larger. This is because the K value for paper is one order of magnitude larger, indicating that wood, drywall, and carpet saturate with contaminant vapors over the time period, while paper does not. Cinderblock has a further order of magnitude larger K value, thus is even further away from being saturated, which is consistent with its even faster sorption rate.

18

Next we consider the overpressurzation period (25-49 hours). Again we see here that wood, drywall, and carpet behave the similarly. This means that these reach the new contaminant saturation equilibrium at roughly the same time.

Here it is important to note that due to diffusion dominated transport through the foundation crack, even though the building is overpressurized, there is still substantial contaminant entry. And because the sole contaminant source is contaminated groundwater, the sorbed equilibrium is determined by this entry rate.

Paper and cinderblock initially behave very similarly during the overpressurization period and desorb contaminants quickly. However, paper reaches its saturation limit after a relatively short time, while cinderblock has not even at the end of the overpressurization cycle. Since the desorption rate constants k_2 are relatively similar for the materials, this disparity is primarily due to the different sorption equilibrium constants K.

Lastly, we consider the final period where the pressurization goes back to its initial state (49-72 hrs). Here we see that the reference case does not quite return to the initial indoor concentration. Thus the contaminant entry rate has not equilibrated yet, because the soil contaminant concentration has not done so either. As in the previous analysis we again see that the wood, drywall, and carpet cases don't differ from the reference. Paper is slightly different, for the same reasons that have already been discussed. Cinderblock is unique here, as it is releasing contaminants, due to the previous change in contaminant concentration. In other words, it is acting as a significant capacitance in the system.

From this simulation work the varied the effects of sorbing indoor materials are apparent. Most of the tested materials only have a moderate effect on the indoor air contaminant concentration dynamics, with the notable exception of cinderblock, which effectively maintains as pseudo-steady-state. However we also see from the analysis of the sorption dynamics that the desorption and sorption rate constants k_1 and k_2 are less important than the overall sorptive capacity K of the material.

3.4. Indoor Material Sorption And Mitigation

The work done by us and others has shown the large sorptive capacities of various common materials. The desorption of the sorbed contaminants may have significant impact on the apparent efficacy of various mitigation systems. To investigate this we consider a scenario where initially the modeled building

19

is depressurized at -5 Pa and at the start of the simulation some perfect mitigation scheme is implemented and the contaminant entry n_{entry} in (29) goes to zero. We also assume that for each case, the indoor environment contains the same amount of indoor material as described in section 3.3. The air exchange rate is assumed to remain a constant 0.5 per hour for the entire simulation time.

Hence, we can drop n_{ck} in (29) and the equations used to model the indoor concentration becomes:

$$V_{\text{bldg}} \frac{\partial c_{\text{in}}}{\partial t} = A_e c_{\text{in}} V_{\text{bldg}} - r_{\text{sorb}} V_{\text{mat}} \tag{29}$$

$$V_{\text{mat}} \frac{\partial c_{\text{sorb}}}{\partial t} = r_{\text{sorb}} V_{\text{mat}} \tag{30}$$

$$r_{\text{sorb}} = k_1 c_{\text{in}} - k_2 c_{\text{sorb}} \tag{31}$$

This system of ordinary differential equations can be solved analytically. A solution to this is

$$\begin{bmatrix} c_{\text{in}} \\ c_{\text{sorb}} \end{bmatrix} = A \exp\left(\lambda_1 t\right) \vec{v_1} + B \exp\left(\lambda_2 t\right) \vec{v_2} \tag{32}$$

and finding the eigenvalues (λ_1, λ_2) and eigenvectors ($\vec{v_1}$, $\vec{v_2}$) of the system above, allows us to calculate the indoor and sorbed contaminants concentrations through time. A and B are constants found using the initial conditions

$$c_{\text{in}}(t = 0) = c_{\text{in},0} \rightarrow A \tag{33}$$

$$c_{\text{sorb}}(t = 0) = c_{\text{sorb},0} K \rightarrow B \tag{34}$$

where we assume that $c_{\text{in},0} = 2$ $(\mu\text{g/m}^3)$.

The decrease in indoor air concentration (as attenuation factor α) for each case is seen in the top panel of Figure 7. As excepted, when there is no sorbing indoor materials, i.e. our reference case, the indoor concentration decreases log-linearly. We can also see that contaminant desorption from materials maintains a higher indoor air concentration relative to reference, with cinderblock again shown to have the great impact.

Clearly, the contaminant desorption from indoor materials can significantly delay the time that a certain reduction in indoor air concentration after a successful mitigation system has been implemented. In the bottom panel of Figure ?? we quantified the number of hours for a fifty percent, a one, and two orders of magnitude reduction in indoor air concentration to
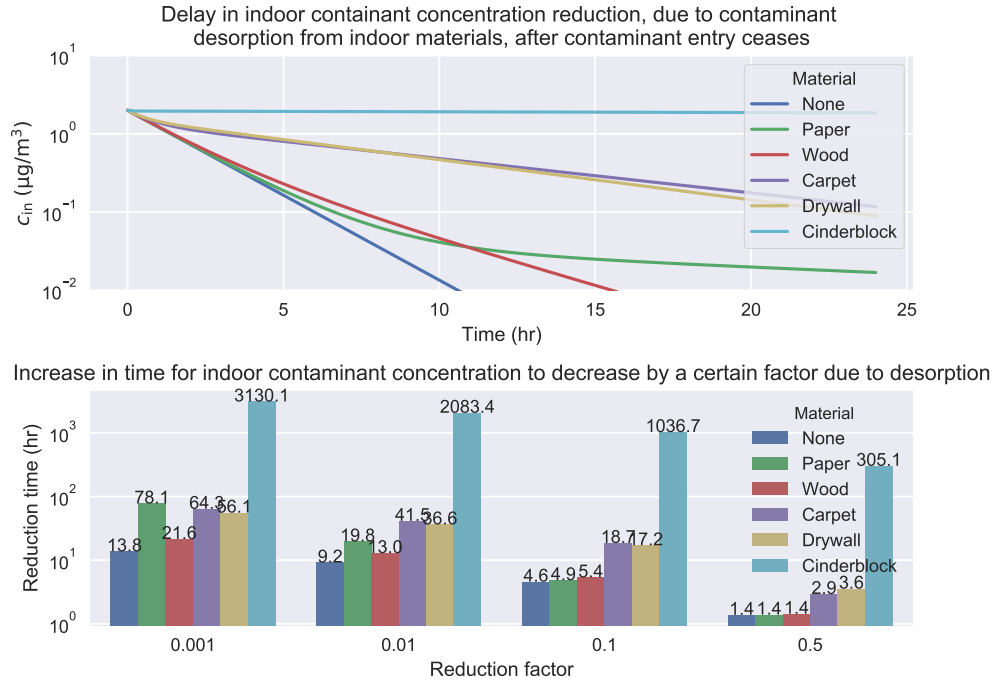
20

Figure 7: Contaminant desorption from indoor materials delay the decrease in indoor contaminant concentration after a mitigation system has been implemented. The top panel shows the indoor air concentration after system implementation, considering desorption from different materials. The bottom panel quantifies how long it takes for the indoor concentration to decrease by a certain factor, considering the different cases.

occurs, both absent sorbing indoor materials (the reference case) and in the presence of the one's presented earlier in this work. On the x-axis the indoor air concentration reduction factor is shown, and on the y-axis the number of hours for the specified reduction occur is displayed, for each material. The number of hours for each case are also shown at the top of each bar.

From this, we see that it takes 1.4 hours for the a 50% reduction in indoor air concentration to occur for the reference, paper, and wood cases, while this time increases up to 305 hours in the cinderblock case. This indicates the significant effect that sorption of TCE onto cinderblock can potentially have on the efficacy on a VI mitigation scheme, with the remaining materials having a relatively minor or moderate effect; a trend we've seen in other parts of this work.

21

4. Conclusions

The work presented here has been some of the first of its kind; exploring how sorption affects VI fundamentally and in some applications. Based on what has been presented here, we can draw some conclusions.

- The sorption and desorption kinetics, while they vary quite a bit, do not seem to make a significant difference in most VI applications or cases, at least not the ones considered here. But, what has been apparent is that it is the sorption capacities of the particular material that matters, although these seem to have to be on the same scale as cinderblock to truly be significant.

- The sorptive capacities of materials vary significantly and it may not be obvious which ones have large sorptive capacities and which do not. More materials, in combination with other contaminants, need to be tested to gain a more comprehensive understanding of which materials are of particular concern in VI.

- Sorption fundamentally retards contaminant transport in soils, effectively increasing the residence time of the contaminant in the soil. However, sorption will only start to retard transport if the sorption partition coefficient is large enough to exceed the "naturally" induced residence by the soil moisture content. Sorption on materials in the indoor environment functions in a similar way, and like a capacitance, inhibits changes in indoor concentration. These particular phenomena may be relevant to consider if one wants to try to influence the contaminant transport and entry rate into the building via forceful pressurization of the building, e.g. the controlled pressure method, as these attempts may be less effective than expected due to sorption.

- Contaminant desorption from indoor materials may also have a significant effect of mitigation systems, potentially delaying effective mitigation from taking place from a matter of hours to several days or weeks, depending on the amount and kind of indoor materials present.

502   Declaration of interest: none

A_{ck}	Crack area
A_e	Air exchange rate
$\alpha,\ n,\ m,\ l$	van Genuchten parameters
α_{gw}	Attenuation from groundwater contaminant vapor source
c_{in}	Indoor air contaminant concentration
c_w	Soil-water contaminant concentration
c_g	Soil-gas contaminant concentration
c_{gw}	Contaminant groundwater concentration
D_{eff}	Effective diffusion coefficient
D_{air}	Diffusion coefficient in air
D_{water}	Diffusion coefficient in water
j_{ck}	Contaminant molar flux through the foundation crack
κ_s	Saturated soil permeability
K_{ads}	Sorption isotherm
K_H	Dimensionless Henry's law constant
k_r	Relative permeability
L_{slab}	Thickness of the foundation slab
M	Molar mass
μ	Contaminant vapor viscosity
p	Pressure in soil
$p_{\mathrm{in/out}}$	Indoor/outdoor pressure difference
ρ	Density
Se	Soil water saturation
t	time
θ_g	Vapor/gas filled porosity
θ_w	Water filled porosity
θ_r	Residual water filled porosity
θ_t	Total porosity
$\vec{u}$	Soil-gas velocity (vector quantity)
VI	Vapor intrusion
V_{base}	Basement volume
z	Elevation above groundwater

Table 4: List of abbreviations and nomenclature

References

[1] R. Meininghaus, L. Gunnarsen, H. N. Knudsen, Diffusion and Sorption of Volatile Organic Compounds in Building Materials-Impact on Indoor Air Quality, Environ. Sci. Technol. 34 (15) (2000) 3101–3108. doi:10.1021/es991291i.

[2] R. Meininghaus, E. Uhde, Diffusion studies of VOC mixtures in a building material, Indoor Air 12 (4) (2002) 215–222. doi:10.1034/j.1600-0668.2002.01131.x.

[3] F. D. Tillman, J. W. Weaver, Review of Recent Research on Vapor Intrusion (2005) 47.

[4] X. Wang, Y. Zhang, J. Xiong, Correlation between the solid/air partition coefficient and liquid molar volume for VOCs in building materials, Atmospheric Environment 42 (33) (2008) 7768–7774. doi:10.1016/j.atmosenv.2008.05.030.

[5] J. Xu, J. S. Zhang, X. Liu, Z. Gao, Determination of partition and diffusion coefficients of formaldehyde in selected building materials and impact of relative humidity, J. Air Waste Manag. Assoc. 62 (6) (2012) 671–679. doi:10.1080/10962247.2012.665812.

[6] A. Bodalal, J. S. Zhang, E. G. Plett, A method for measuring internal diffusion and equilibrium partition coefficients of volatile organic compounds for building materials, Building and Environment 35 (2) (2000) 101–110. doi:10.1016/S0360-1323(99)00005-0.

[7] U.S. Environmental Protection Agency, OSWER Technical Guide for Assessing and Mitigating the Vapor Intrusion Pathway From Subsurface Vapor Sources To Indoor Air (2015).

[8] C. Holton, Y. Guo, H. Luo, P. Dahlen, K. Gorder, E. Dettenmaier, P. C. Johnson, Long-Term Evaluation of the Controlled Pressure Method for Assessment of the Vapor Intrusion Pathway, Environ. Sci. Technol. 49 (4) (2015) 2091–2098. doi:10/f64j45.

[9] C. C. Lutes, R. S. Truesdale, B. W. Cosky, J. H. Zimmerman, B. A. Schumacher, Comparing Vapor Intrusion Mitigation System

Performance for VOCs and Radon, Remediation 25 (4) (2015) 7–26. doi:10/gd6dfn.

[10] U.S. Environmental Protection Agency, Assessment of Mitigation Systems on Vapor Intrusion: Temporal Trends, Attenuation Factors, and Contaminant Migration Routes under Mitigated And Non-mitigated Conditions (2015).

[11] T. McHugh, P. Loll, B. Eklund, Recent advances in vapor intrusion site investigations, Journal of Environmental Management 204 (2017) 783–792. doi:10/gd6dgk.

[12] R. Shen, K. G. Pennell, E. M. Suuberg, A numerical investigation of vapor intrusion — The dynamic response of contaminant vapors to rainfall events, Science of The Total Environment 437 (2012) 110–120. doi:10/f4fp9s.

[13] J. G. V. Ström, Y. Guo, Y. Yao, E. M. Suuberg, Factors affecting temporal variations in vapor intrusion-induced indoor air contaminant concentrations, Building and Environment 161 (2019) 106196. doi:10.1016/j.buildenv.2019.106196.

[14] M. T. van Genuchten, A Closed-form Equation for Predicting the Hydraulic Conductivity of Unsaturated Soils, Soil Sci. Soc. Am. 44 (5) (1980) 892–898. doi:10/fdc8mc.

[15] E. Jones, T. Oliphant, Pearu Peterson, SciPy: Open source scientific tools for Python (2011).

[16] L. D. V. Abreu, H. Schuver, Conceptual Model Scenarios for the Vapor Intrusion Pathway (2012).

[17] U.S. Environmental Protection Agency, Users's Guide For Evaluating Subsurface Vapor Intrusion Into Buildings (2004).